Journal of Ultrafine Grained and Nanostructured Materials
https://jufgnsm.ut.ac.ir
Vol. 57, No.2, December 2024, pp. 158-167
Print ISSN: 2423-6845 Online ISSN: 2423-6837
DOI: 10.22059/jufgnsm.2024.02.06

Green Synthesis and Characterization of $Cu_{0.5}Zn_{0.5}FeAlO_4$ Magnetic Nanoparticles with Enhanced Photocatalytic Activity

Husam Abdulhussein Radhi Alzuabidi, Ali Naghipour*, Saeid Taghavi Fardood*

Department of Chemistry, Faculty of Science, Ilam University, Ilam 69315516, Iran

Recieved: 2 December 2024; Accepted: 15 December 2024

**Corresponding authors, Ali Naghipour:* (a.naghipour@ilam.ac.ir); Saeid Taghavi Fardood:(s.taghavi@ilam.ac.ir)

ABSTRACT

Water pollution poses a significant global challenge, with toxic and carcinogenic dyes in wastewater threatening human health. Developing efficient and reusable photocatalysts is essential for advanced and sustainable water treatment solutions. In this project, Magnetic $Cu_{0.5}Zn_{0.5}FeAlO_4$ nanoparticles were prepared through an eco-friendly method utilizing tragacanth gel as a stabilizing agent. The resulting nanoparticles were characterized using XRD, BET, FESEM, UV–Vis-DRS, TEM, EDX, Mapping and VSM techniques. The XRD pattern confirms the presence of the cubic spinel crystal structure in the $Cu_{0.5}Zn_{0.5}FeAlO_4$ MNPs, with an average crystallite size of 12 nm. The TEM image showed an average particle size of 25–30 nm. The EDX and mapping analysis reveal all elemental compositions in $Cu_{0.5}Zn_{0.5}FeAlO_4$ MNPs, indicating a pure phase. The band gap was determined from UV–vis DRS spectra by using the tauc equation and it was found to be of about 1.95 ev. The VSM analysis demonstrated superparamagnetic properties with a saturation magnetization value of approximately 3.74 emu/g. The $Cu_{0.5}Zn_{0.5}FeAlO_4$ MNPs exhibited efficient photodegradation of reactive blue 222 dye when under visible light. The sample was easily recovered and reused due to the magnetic properties of the nanoparticles. This showed excellent catalytic efficiency, maintaining strong performance for up to four cycles with very little loss in activity.

Keywords: *Green synthesis, Magnetic naoparticles, Reactive blue 222 degradation, Photocatalysis.*

1. Introduction

Environmental pollution is increasing, and the world is becoming more attuned to the conservation of natural resources [1, 2]. The effluent from the textile industry is a complicated amalgamation of chemicals that fluctuates in both quality and quantity. It generates organic and inorganic waste that might alter chemical and biological parameters, while dye effluent may lead to observable environmental impacts [3-5]. Dyes and colored effluents can produce toxic, carcinogenic substances that contaminate water, constituting a significant offense. Ion exchange, chemical precipitation, and filtration are costly techniques for dye removal from water, potentially converting dyes into secondary contaminants necessitating additional treatment [6-12]. Adsorption is a low-cost, efficient technique for dye removal, offering advantages such as simplicity, adaptability, and ease of operation, though it may also produce secondary pollutants [13, 14]. The semiconductor photo-catalysts degrade organic compounds, chemicals, and dyes under light [15-17]. This method was acceptable and effective for degrading several harmful elements, such as organic and aquatic pollutants, giving it substantial advantages over the old method [18-20].

In ferrite components, the substitution of

magnetic and non-magnetic ions at various sublattices has led to interesting magnetic configurations and electrical characteristics [21]. Ferrites exhibit notable characteristics due to magnetic instability and frustration. Exchange contact competition results in unmet bonds, leading to magnetic dilution and diverse structures [22-26]. The magnetic and electrical characteristics of the spinel lattice are influenced by nonmagnetic ions. Isomorphous interactions in iron oxides diminish magnetic interactions, magnetic ordering temperatures, and magnetic-field super transfer. Al^{3+} ions in aluminum-substituted ferrites preferentially occupy the octahedral B-site [27-31]. Various techniques have been described for the production of magnetic nanoparticles, including sol-gel, hydrothermal, co-precipitation, and sonochemical processes [32- 34]. Numerous approaches demonstrate drawbacks, such as high expenses, substantial energy usage, pollution from chemical precursors, and the production of toxic byproducts. The eco-friendly production of magnetic nanoparticles using plant extracts offers a viable alternative to chemical approaches, with polyphenols acting as natural reducing agents [35-37].

In the current work, $Cu_{0.5}Zn_{0.5}FeAlO_4$ was synthesized using a simple green technique. The morphology, structure, and optical properties were examined and described. The photocatalytic performance of the magnetic nanoparticles in degrading reactive blue 222 dye (Fig. 1) was investigated and reported.

2. Experimental

2.1. Chemicals

Tragacanth gel (TG) was purchased from a nearby health food store. The all metal salts were obtained from Merck.

2.2. Green synthesis of $Cu_{0.5}Zn_{0.5}FeAlO_4$ MNPs

$Cu_{0.5}Zn_{0.5}FeAlO_4$ MNPs were synthesized in a one-step green process following the previously described method [39]. The TG was first dissolved in distilled water to form a clear gel. Stoichiometric amounts of $Cu(NO_3)_2{\cdot}3H_2O$, $Zn(NO_3)_2{\cdot}6H_2O$, $Al(NO_3)_3{\cdot}9H_2O$, and $Fe(NO_3)_3{\cdot}9H_2O$ were then added to the gel, and the mixture was maintained at 75°C with continuous stirring for 10 h. The product was subsequently annealed at 600°C for 4 hours to obtain $Cu_{0.5}Zn_{0.5}FeAlO_4$ MNPs.

2.3. Photocatalytic activity evaluation

The photocatalytic performance of $Cu_{0.5}Zn_{0.5}FeAlO_4$ MNPs was evaluated by the photodegradation of reactive blue 222 dye under visible light. All procedures were performed in a photoreactor, with visible light supplied by a fluorescent lamp ($\lambda > 400$ nm, 80 W, Delta, Iran). To identify optimal degradation conditions, several concentrations of RB 222, MNPs amounts, and contact durations were evaluated. At specified intervals, a sample was taken, and the MNPs were separated using a magnetic field. Absorbance changes at $\lambda_{max} = 612$ nm were measured using the UV–Vis technique to monitor RB 222 degradation. The degradation rates of RB 222 were later determined utilizing the following formula:

$$\%\ Degradation = \frac{A_0 - A_t}{A_0} \times 100$$

3. Results and discussion

3.1. Characterization

XRD analysis was performed to characterize the synthesized MNPs, and the results are shown in Fig. 2. The diffraction peaks observed correspond to the cubic spinel phase of $Cu_{0.5}Zn_{0.5}FeAlO_4$ as identified by JCPDS Card No. 82-1040. The sharp and narrow diffraction peaks indicate the high crystallinity of the nanoparticles. The crystallite size of $Cu_{0.5}Zn_{0.5}FeAlO_4$ MNPs was estimated using the Scherrer equation [40], and the calculated value was 12 nm.

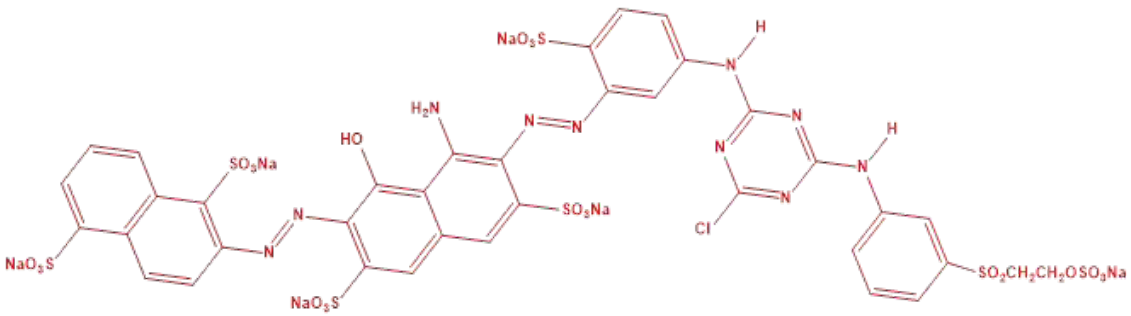

Fig. 1- Structure of RB222 [38].

The morphology of $Cu_{0.5}Zn_{0.5}FeAlO_4$ MNPs was studied using FESEM, as shown in Fig. 3a. It was determined that the synthesized nanoparticles exhibit spherical and irregular morphological characteristics. TEM analysis (Fig. 3b) was carried out to provide further evidence on the structural information of $Cu_{0.5}Zn_{0.5}FeAlO_4$ MNPs. The TEM image of the nanoparticles shows average particle sizes of 25-30 nm.

In addition, EDX analysis (Fig. 4) provided conclusive evidence of the presence of iron (Fe), aluminum (Al), copper (Cu), zinc (Zn), and oxygen (O) as the primary components of the sample. The Mapping analysis (Fig. 4) also confirmed the material's structural integrity and elemental distribution.

Figure 5 illustrates the magnetization measurements of $Cu_{0.5}Zn_{0.5}FeAlO_4$ magnetic nanoparticles. The VSM curve shows that both the remanence (Mr) and coercivity (Hc) are zero, indicating superparamagnetic behavior. The saturation magnetization (Ms) is 3.74 emu/g, signifying the magnetic properties of the nanoparticles.

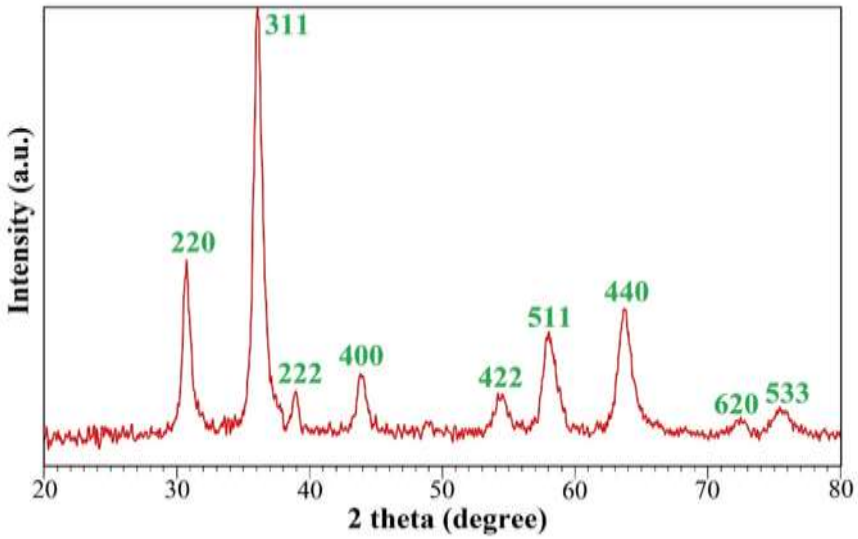

Fig. 2- XRD pattern of $Cu_{0.5}Zn_{0.5}FeAlO_4$ MNPs.

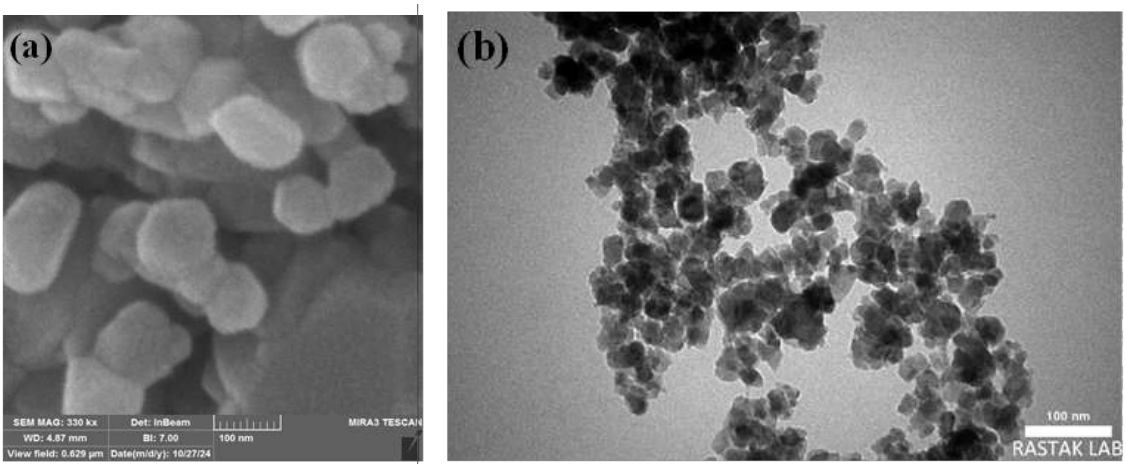

Fig. 3- a) FESEM image and b) TEM image of $Cu_{0.5}Zn_{0.5}FeAlO_4$ MNPs.

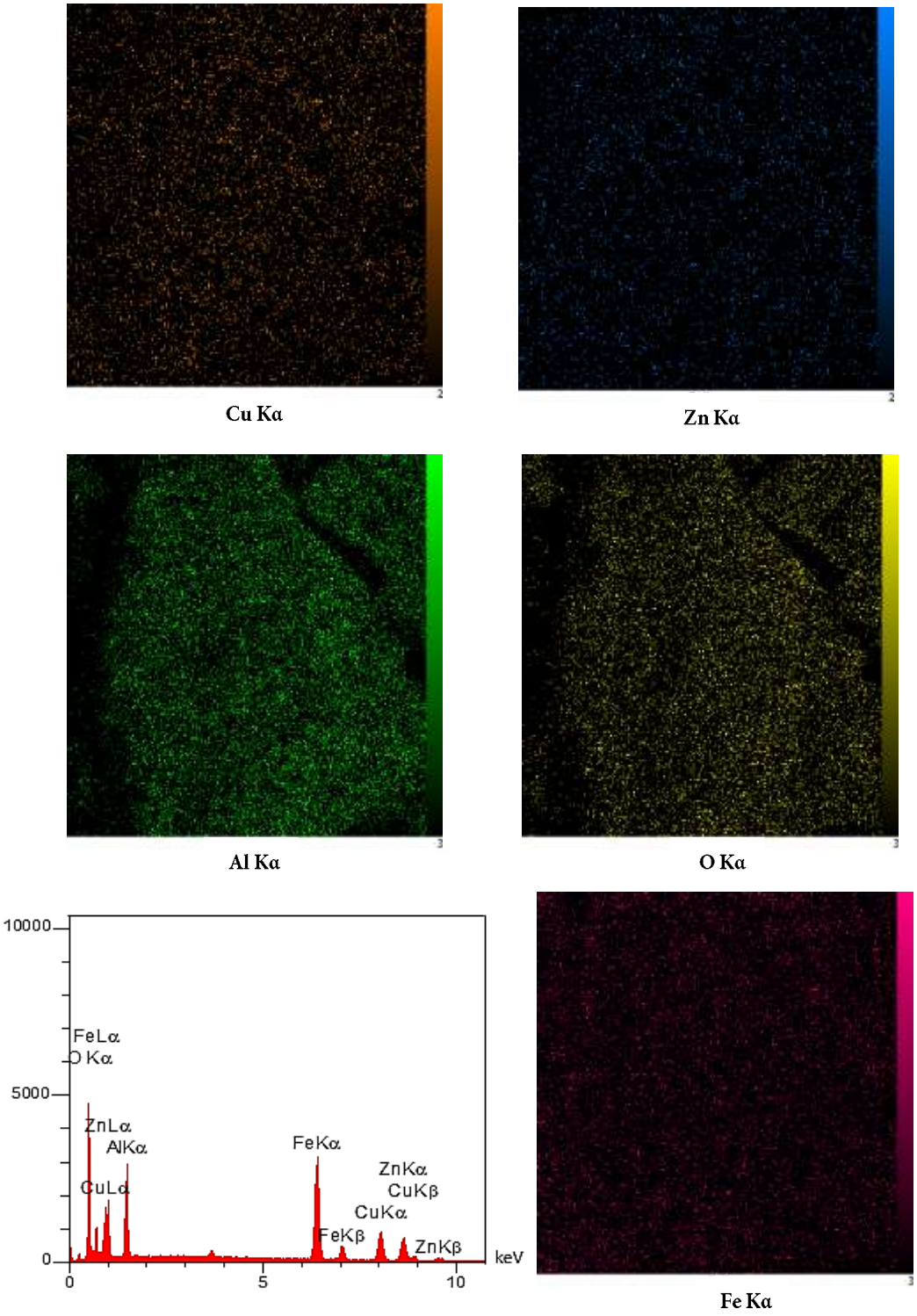

Fig. 4- EDX pattern and elemental mapping of $Cu_{0.5}Zn_{0.5}FeAlO_4$ MNPs.

The N_2 adsorption-desorption isotherms and BJH pore size distribution diagram of $Cu_{0.5}Zn_{0.5}FeAlO_4$ MNPs are shown in Figure 6. Fig. 6a shows the usual IUPAC classifications of type IV isotherms, which indicate a uniform pore size distribution in mesoporous materials. Surface analysis by BET showed a value of 46.348 m^2g^{-1}. In Figure 6b, the BJH equation indicates that the nanoparticles have pores with a size of 6.06 nm [41].

The UV-Vis-DRS and Tauc plot of the synthesized $Cu_{0.5}Zn_{0.5}FeAlO_4$ MNPs is shown in Figure 7. The band gap of the material is clearly seen to be around 1.95 eV from the graph. This result suggests the nanoparticles have suitable bandgap for visible-light photocatalysis and are potential photocatalytic candidates.

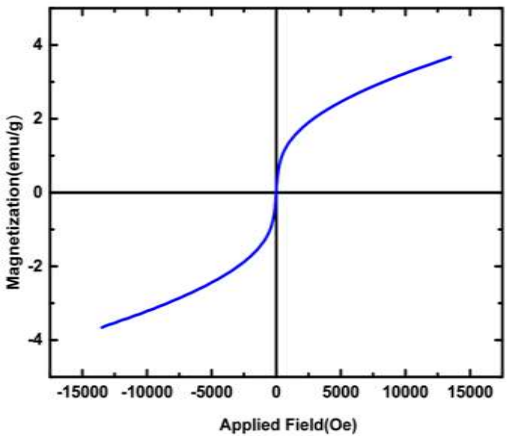

Fig. 5- VSM curve of $Cu_{0.5}Zn_{0.5}FeAlO_4$ NPs.

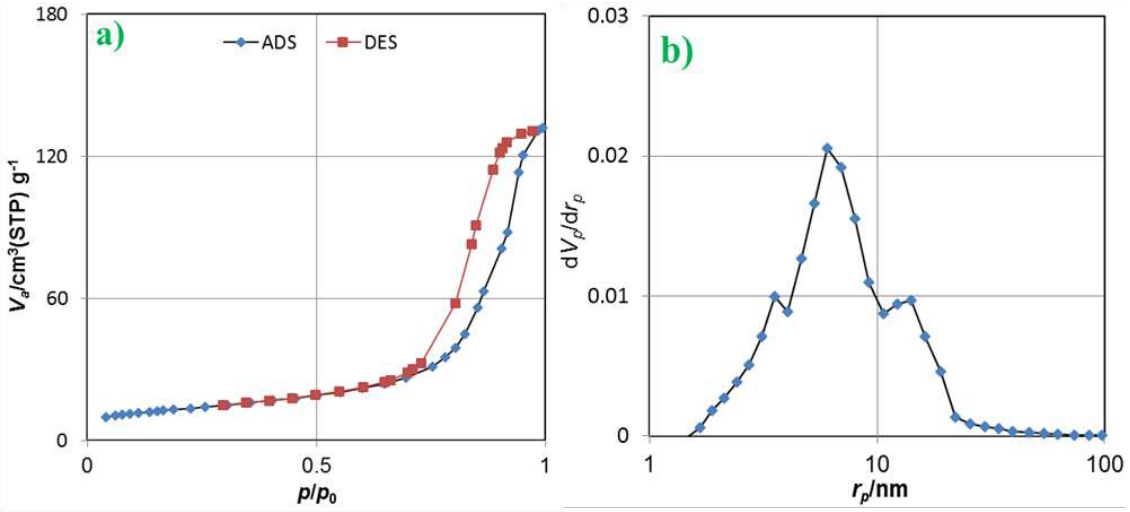

Fig. 6- a) The N_2 absorption/desorption isotherm b) BJH diagram of $Cu_{0.5}Zn_{0.5}FeAlO_4$ NPs.

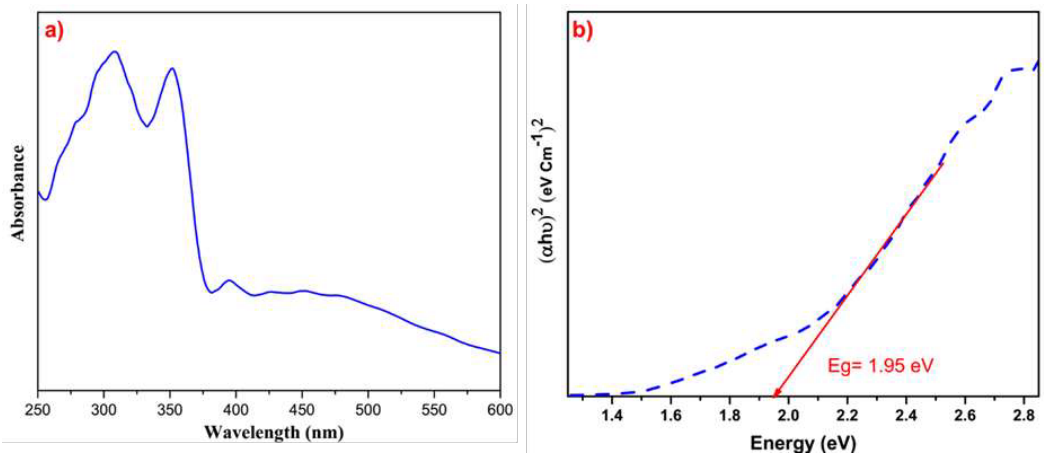

Fig. 7- a) UV-Vis-DRS and b) Tauc plot of $Cu_{0.5}Zn_{0.5}FeAlO_4$ MNPs.

3.2. Photocatalytic Activity of $Cu_{0.5}Zn_{0.5}FeAlO_4$ MNPs

Figure 8a indicates that raising the quantity of $Cu_{0.5}Zn_{0.5}FeAlO_4$ MNPs from 0.02 to 0.04 g enhanced degradation efficiency due to an increase in active sites and hydroxyl radical generation. Nevertheless, escalating the dosage to 0.05 g resulted in a very slight and nearly constant decrease in efficiency, possibly attributable to particle aggregation, which diminished the surface area and active sites, thereby attenuating the absorption of light [42]. Consequently, 0.04 g was identified as the optimal dosage.

Figure 8b illustrates the influence of the initial RB222 concentration on degradation efficiency, evaluated at different dye concentrations (10 to 40 mg/L), utilizing 0.04 g of $Cu_{0.5}Zn_{0.5}FeAlO_4$ MNPs and a reaction duration of 45 min. The degradation efficiency decreased as the RB222 dye concentration increased, achieving 79% dye degradation at 40 mg/L. Increased dye concentrations may prevent heat and energy transfer from cavitation, thereby restricting hydroxyl radical generation and diminishing degradation efficiency [43].

The process was investigated under three different conditions to evaluate the photocatalytic activity of $Cu_{0.5}Zn_{0.5}FeAlO_4$ MNPs (Fig 9a). No degradation was observed under photolysis conditions (without MNPs). The catalyst adsorbed 53% of the dye in 45 min when evaluated without visible light. However, in the presence of visible light, the photocatalytic performance was 95% dye degradation, which indicates that magnetic nanoparticles significantly enhance degradation under visible light. Experiments were conducted using fixed concentrations of $Cu_{0.5}Zn_{0.5}FeAlO_4$ MNPs and RB 222 under photocatalytic conditions to optimize the degradation time. After 45 min of visible-light irradiation, the absorbance of the RB 222 dye significantly decreased, achieving 95% degradation (Fig 9b). Additionally, TOC analysis revealed 63% reduction, highlighting the high efficiency of the photocatalytic process.

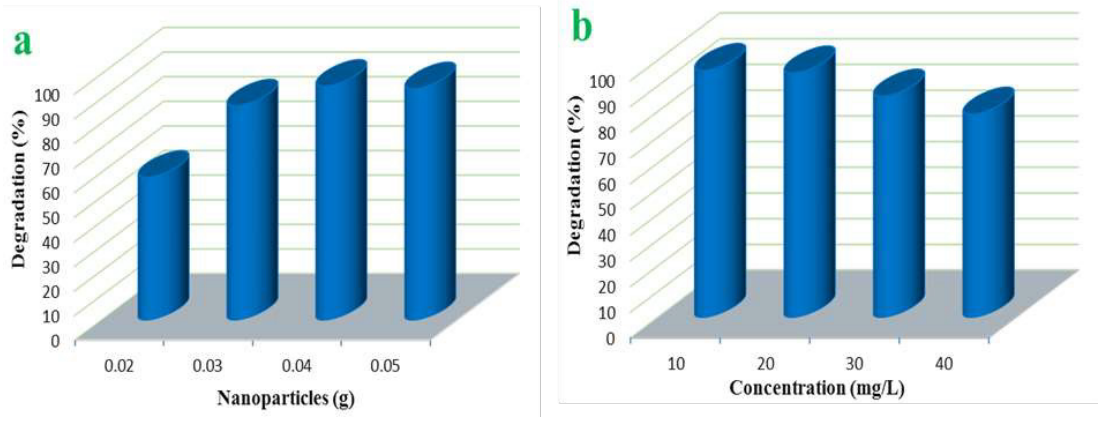

Fig. 8- The effect of a) $Cu_{0.5}Zn_{0.5}FeAlO_4$ amount b) RB 222 concentration.

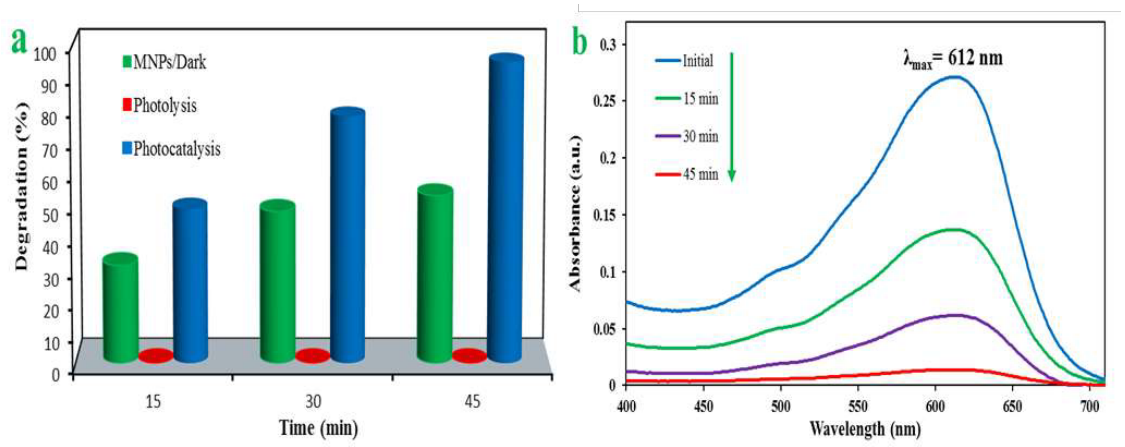

Fig. 9- a) Effect of visible light irradiation b) UV-Vis spectrum of RB 222 Dye during degradation.

A cyclic photocatalysis assessment was conducted over four iterations to determine the stability and reusability of the produced $Cu_{0.5}Zn_{0.5}FeAlO_4$ MNPs (Fig. 10). Following each cycles, the nanoparticles were separated using magnet and washed with water prior to their reutilization in the subsequent run. The findings indicated that the nanoparticles effectively destroy RB222 dye.

The photocatalyst produces h^+, $O_2\bullet^-$, and •OH, which are responsible for dye degradation [44, 45]. In an effort to learn more about the photocatalytic process and active species, active-species trapping experiments were performed. The addition of ethanol (•OH scavenger) and EDTA (h^+ scavenger) reduced the degradation of RB222 to 52% and 61%, respectively (Fig. 11). The addition of benzoquinone (BQ) as an $O_2\bullet^-$ scavenger had a minor effect on the degradation. The results indicate that •OH is the main active species, while h^+ acts as a cofactor and plays a secondary role in dye degradation.

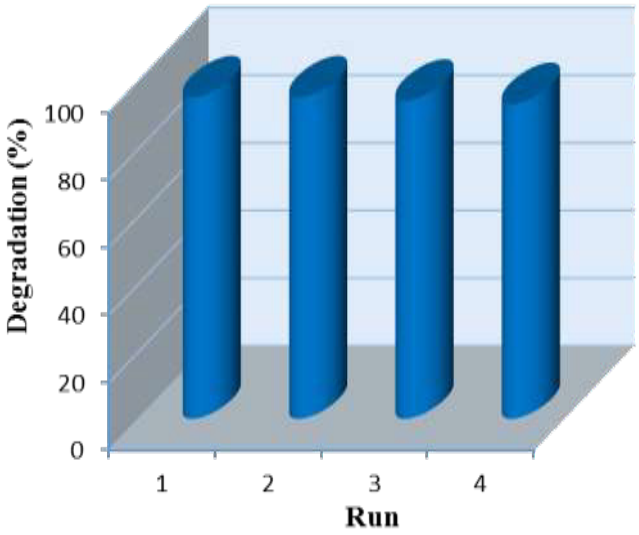

Fig. 10- Reusability of $Cu_{0.5}Zn_{0.5}FeAlO_4$ MNPs.

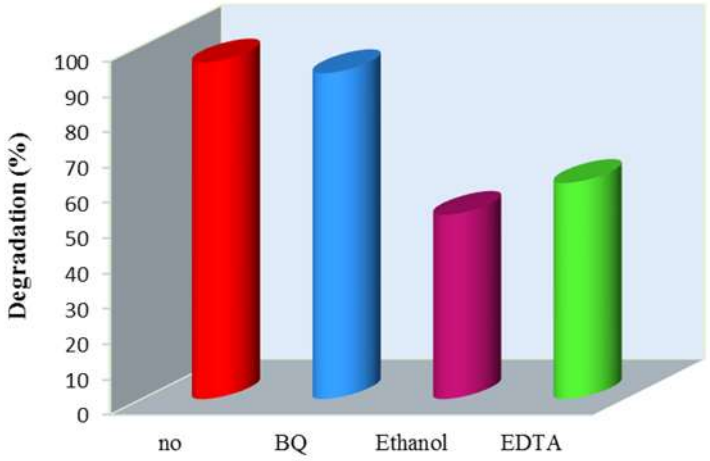

Fig. 11- The Effect of Scavengers on RB222 Degradation.

Compared to other photocatalysts, $Cu_{0.5}Zn_{0.5}FeAlO_4$ nanoparticles degraded more efficiently and took less time to react (Table 1). Such nanoparticles also have some unique benefits such as superparamagnetic recovery and reuse, which make them ideally suited for applications. Moreover, they cannot be produced using toxic chemicals or solvents. Their sustainability is improved by this green, simple synthesis, which stands out from other catalysts that would otherwise require toxic reagents. Ultimately, $Cu_{0.5}Zn_{0.5}FeAlO_4$ nanoparticles deliver high photocatalytic activity, magnetic separability, and nontoxic synthesis, making them attractive candidates for environmentally sound applications.

4. Conclusions

In conclusion, the eco-friendly synthesized magnetic $Cu_{0.5}Zn_{0.5}FeAlO_4$ nanoparticles demonstrated excellent photocatalytic performance, achieving 95% degradation of reactive blue 222 dye under visible light irradiation within 45 minutes. The photocatalytic degradation was primarily driven by hydroxyl radicals (•OH) and holes (h^+), which played key roles in breaking down the dye. TOC analysis demonstrated a 63% reduction in total organic carbon, further confirming the effectiveness of the photocatalytic process. Additionally, the nanoparticles exhibited strong stability, maintaining high performance with minimal loss in activity over four cycles due to their magnetic properties, which allowed for easy recovery and reuse. This makes $Cu_{0.5}Zn_{0.5}FeAlO_4$ nanoparticles a promising candidate for sustainable environmental applications.

References

1. Kumari H, Sonia, Suman, Ranga R, Chahal S, Devi S, Sharma S, Kumar S, Kumar P, and Kumar S, A review on photocatalysis used for wastewater treatment: dye degradation. Water, Air, & Soil Pollution. 2023;234:349.
2. Al Taee MB and Al Shabander BM, Study the Effect of ZnO Concentrations on The Photocatalytic Activity of TiO_2/Cement Nanocomposites. Chemical Methodologies. 2022;6:831-841.
3. AbouSeada N, Ahmed MA, and Elmahgary MG, Synthesis and characterization of novel magnetic nanoparticles for photocatalytic degradation of indigo carmine dye. Materials Science for Energy Technologies. 2022;5:116-124.
4. Saadati A and Sheibani S, Photocatalytic performance of SnS_2 nanoflakes synthesized through a facile reflux method. Journal of Ultrafine Grained and Nanostructured Materials. 2023;56:129-136.
5. Hadi E and Jasim KK, Responsive UV-light Photocatalytic of Ag/ZnO Nanocomposites for Removal of Brilliant Blue Dye: As a Model for Advanced Chemical Studies. Advanced Journal of Chemistry, Section A. 2024;604-614.
6. Moalej NS, Ahadi S, and Sheibani S, Photocatalytic degradation of methylene blue by 2 wt.% Fe doped TiO_2 nanopowder under visible light irradiation. Journal of Ultrafine Grained and Nanostructured Materials. 2019;52:133-141.
7. Arjomandi Rad F and Talat Mehrabad J, Exploring the Photocatalytic Activity of Magnesium and Copper-Doped Titanium Dioxide Nano Catalyst through Synthesis and Characterization. Advanced Journal of Chemistry, Section A. 2024;7:374-385.
8. Vishnu G, Singh S, Naik TSK, Viswanath R, Ramamurthy PC, Bhadrecha P, Naik HB, Singh J, Khan NA, and Zahmatkesh S, Photodegradation of methylene blue dye using light driven photocatalyst-green cobalt doped cadmium ferrite nanoparticles as antibacterial agents. Journal of Cleaner Production. 2023;404:136977.
9. Taghavi Fardood S, Moradnia F, and Aminabhavi TM, Green synthesis of novel $Zn_{0.5}Ni_{0.5}FeCrO_4$ spinel magnetic nanoparticles: Photodegradation of 4-nitrophenol and aniline under visible light irradiation. Environmental Pollution. 2024;358:124534.
10. Gumma S, Puthalapattu RP, Punyasamudram S, Kanuparthy

Table 1- Comparison of RB 222 degradation with other catalysts.

Catalysts	Methods	Light	Time (min)	Degradation rate (%)	Refs.
ZnO	**Commercial**	**UV**	**120**	**80**	**[46]**
Fe_2O_3/Mn_2O_3/ $FeMn_2O_4$	**Chemical**	**Solar**	**110**	**82**	**[47]**
Magnetic sodium alginate beads/(H_2O_2)	**Chemical**	**-**	**180**	**95**	**[48]**
MnO_x@PVDF/ MWCNTs	**Hydrothermal**	**Visible**	**30**	**68.7**	**[49]**
Al_2O_3/ZrO_2	**Green**	**Visible**	**60**	**91**	**[50]**
$Cu_{0.5}Zn_{0.5}Fe_2O_4$	**Green**	**Visible**	**45**	**90**	**[51]**
$Cu_{0.5}Zn_{0.5}FeAlO_4$	**Green**	**Visible**	**45**	**95**	**This work**

PR, and Putta Venkata NK, Eco-Friendly Phytochemical-Derived Co_3O_4@Ag Nanoparticles for Ethanol Oxidation and Antibacterial Activity. Asian Journal of Green Chemistry. 2024;8:560-578.
11. Hakimi M, Hosseini HA, and Elhaminezhad B, Fabrication of Manganese Dioxide Nanoparticles in Starch and Gelatin Beds: Investigation of Photocatalytic Activity. Chemical Methodologies. 2023;8:37-46.
12. Chala GH, Review on Green Synthesis of Iron-Based Nanoparticles for Environmental Applications. Journal of Chemical Reviews. 2023;5:1-14.
13. Jalali N, Nami M, Rashchi F, and Rakhsha A, Photocatalytic properties of ZnO/CuO nanocomposite prepared in acidic media. Journal of Ultrafine Grained and Nanostructured Materials. 2022;55:21-30.
14. Taghavi Fardood S, Moradnia F, Yekke Zare F, Heidarzadeh S, Azad Majedi M, Ramazani A, Sillanpää M, and Nguyen K, Green synthesis and characterization of α-Mn_2O_3 nanoparticles for antibacterial activity and efficient visible-light photocatalysis. Scientific reports. 2024;14:6755.
15. Ansari F, Sheibani S, Caudillo-Flores U, and Fernández-García M, Effect of calcination process on the gas phase photodegradation by CuO-Cu_2O/TiO_2 nanocomposite photocatalyst. Journal of Ultrafine Grained and Nanostructured Materials. 2020;53:23-30.
16. Scaria SS and Sebastian JK, Novel biocompatible zinc oxide nanoparticle synthesis using Quassia indica leaf extract and evaluation of its photocatalytic, antimicrobial, and cytotoxic potentials. Biomass Conversion and Biorefinery. 2023;1-20.
17. Bashar MA, Molla MTH, Chandra D, Malitha MD, Islam MS, Rahman MS, and Ahsan MS, Hydrothermal synthesis of cobalt substitute zinc-ferrite ($Co_{1-x}Zn_xFe_2O_4$) nanodot, functionalised by polyaniline with enhanced photocatalytic activity under visible light irradiation. Heliyon. 2023;9:
18. Mohamed A, Mahanna H, and Samy M, Synergistic effects of photocatalysis-periodate activation system for the degradation of emerging pollutants using GO/MgO nanohybrid. Journal of Environmental Chemical Engineering. 2024;12:112248.
19. Singh S, Atri AK, Qadir I, Sharma S, Manhas U, and Singh D, Role of different fuels and sintering temperatures in the structural, optical, magnetic, and photocatalytic properties of chromium-containing nickel ferrite: kinetic study of photocatalytic degradation of rhodamine B dye. ACS Omega. 2023;8:6302-6317.
20. Singh J, Kumari P, and Basu S, Degradation of toxic industrial dyes using SnO_2/g-C_3N_4 nanocomposites: Role of mass ratio on photocatalytic activity. Journal of Photochemistry and Photobiology A: Chemistry. 2019;371:136-143.
21. Sarmah S, Patra K, Maji P, Ravi S, and Bora T, A comparative study on the structural, magnetic and dielectric properties of magnesium substituted cobalt ferrites. Ceramics International. 2023;49:1444-1463.
22. Ahmad I, Abbas T, Ziya AB, Abbas G, and Maqsood A, Size dependent structural and magnetic properties of Al substituted Co–Mg ferrites synthesized by the sol–gel auto-combustion method. Materials Research Bulletin. 2014;52:11-14.
23. Okba EA, Fakhry FE, El-Bahnasawy HH, Abdel-Galeil MM, and El Shater RE, Development of heterogeneous photocatalysis delafossite structured Ag doped Cd-Cu ferrite spinel nanoparticles for an efficient photodegradation process. Journal of Photochemistry and Photobiology A: Chemistry. 2024;448:115275.
24. Harki DAH, Naghipour A, and Taghavi Fardood S, Eco-Friendly Synthesis and Characterization of $Mg_{0.5}Co_{0.5}Fe_2O_4$ Magnetic Nanoparticles for Photocatalytic Degradation of Congo Red Dye. Case Studies in Chemical and Environmental Engineering. 2024;10:101016.
25. Shafiq K, Aadil M, Hassan W, Choudhry Q, Gul S, Rais A, Fattah AA, Mahmoud KH, and Ansari MZ, Cobalt and holmium co-doped nickel ferrite nanoparticles: synthesis, characterization and photocatalytic application studies. Zeitschrift fur Physikalische Chemie. 2023;237:1325-1344.
26. Sarifuddin WS, Mahadi AH, Hussin MR, Masri MKZ, Prasetyoko D, and Bahruji H, Cu doped $ZnFe_2O_4$ photocatalysts for enhanced hydrogen production and dye degradation in the visible region. Journal of Photochemistry and Photobiology A: Chemistry. 2024;453:115658.
27. Singhal S, Barthwal SK, and Chandra K, Structural, magnetic and Mössbauer spectral studies of nanosize aluminum substituted nickel zinc ferrites. Journal of Magnetism and Magnetic Materials. 2006;296:94-103.
28. Henderson CMB, Charnock JM, and Plant DA, Cation occupancies in Mg, Co, Ni, Zn, Al ferrite spinels: a multi-element EXAFS study. Journal of Physics: Condensed Matter. 2007;19:076214.
29. Yasar M and Kadhem AA, Investigating the Role of Aluminum Doping on the Bandgap Modulation and Photocatalytic Efficiency of Strontium Nickel Ferrites for Ciprofloxacin Degradation. Arabian Journal for Science and Engineering. 2024;1-15.
30. Yasar M, Nazir R, and Noreen F, Synthesis, characterization, and photocatalytic activity of aluminum-doped nickel manganese ferrite for the photodegradation of methylene blue. Reaction Kinetics, Mechanisms and Catalysis. 2024;137:505-521.
31. Ramadevi P, Shanmugavadivu R, Venkatesan R, Mayandi J, and Sagadevan S, Photocatalytic dye degradation efficiency and reusability of aluminium substituted nickel ferrite nanostructures for wastewater remediation. Inorganic Chemistry Communications. 2023;150:110532.
32. Abidin MZU, Ikram M, Moeen S, Nazir G, Kanoun MB, and Goumri-Said S, A comprehensive review on the synthesis of ferrite nanomaterials via bottom-up and top-down approaches advantages, disadvantages, characterizations and computational insights. Coordination Chemistry Reviews. 2024;520:216158.
33. Dichayal S, Murade V, Deshmukh S, Pansambal S, Hase D, and Oza R, Green Synthesis of Cobalt Ferrite Nanoparticles: A Comprehensive Review on Eco-friendly Approaches, Characterization Techniques, and Potential Applications. Journal of Chemical Reviews. 2024.
34. Slimani Y and Hannachi E, Synthesis of ferrite nanoparticles using sonochemical methods, in Ferrite Nanostructured Magnetic Materials. 2023, Elsevier. p. 121-147.
35. Tamboli QY, Patange SM, Mohanta YK, Sharma R, and Zakde KR, Green synthesis of cobalt ferrite nanoparticles: An emerging material for environmental and biomedical applications. Journal of Nanomaterials. 2023;2023:9770212.
36. Kurian M, Green synthesis routes for spinel ferrite nanoparticles: a short review on the recent trends. Journal of the Australian Ceramic Society. 2023;59:1161-1175.
37. Fiaz S, Ahmed MN, ul Haq I, Shah SWA, and Waseem M, Green synthesis of cobalt ferrite and Mn doped cobalt ferrite nanoparticles: Anticancer, antidiabetic and antibacterial studies. Journal of Trace Elements in Medicine and Biology. 2023;80:127292.
38. Sherin A, Munir R, Mushtaq N, Muneer A, Ambreen H, Younas F, Farah MA, Elsadek MF, and Noreen S, Reactive Blue MEBF 222 dye and textile wastewater treatment using metal-doped cobalt and nickel perovskites by batch and column adsorption process. Environmental Monitoring and Assessment. 2024;196:927.

39. Kiani MT, Ramazani A, and Taghavi Fardood S, Green synthesis and characterization of $Ni_{0.25}Zn_{0.75}Fe_2O_4$ magnetic nanoparticles and study of their photocatalytic activity in the degradation of aniline. Applied Organometallic Chemistry. 2023;37:e7053.
40. Ahankar H, Taghavi Fardood S, and Ramazani A, One-pot three-component synthesis of tetrahydrobenzo[b]pyrans in the presence of $Ni_{0.5}Cu_{0.5}Fe_2O_4$ magnetic nanoparticles under microwave irradiation in solvent-free conditions. Iranian Journal OF Catalysis. 2020;10:195-201.
41. Kiani MT, Ramazani A, Rahmani S, and Taghavi Fardood S, Green synthesis and characterisation of superparamagnetic $Cu_{0.25}Zn_{0.75}Fe_2O_4$ nanoparticles and investigation of their photocatalytic activity. International Journal of Environmental Analytical Chemistry. 2024;104:2895-2911.
42. Taghavi Fardood S, Moradnia F, Forootan R, Abbassi R, Jalalifar S, Ramazani A, and Sillanpää M, Facile green synthesis, characterization and visible light photocatalytic activity of $MgFe_2O_4$@$CoCr_2O_4$ magnetic nanocomposite. Journal of Photochemistry and Photobiology A: Chemistry. 2022;423:113621.
43. Taghavi Fardood S, Ganjkhanlu S, Moradnia F, and Ramazani A, Green synthesis, characterization, and photocatalytic activity of superparamagnetic $MgFe_2O_4$@$ZnAl_2O_4$ nanocomposites. Scientific reports. 2024;14:16670.
44. Das GS, Shim JP, Bhatnagar A, Tripathi KM, and Kim T, Biomass-derived Carbon Quantum Dots for Visible-Light-Induced Photocatalysis and Label-Free Detection of Fe(III) and Ascorbic acid. Scientific reports. 2019;9:15084.
45. Zheng X, Yuan J, Shen J, Liang J, Che J, Tang B, He G, and Chen H, A carnation-like rGO/$Bi_2O_2CO_3$/BiOCl composite: efficient photocatalyst for the degradation of ciprofloxacin. Journal of Materials Science: Materials in Electronics. 2019;30:5986-5994.
46. Gouvêa CAK, Wypych F, Moraes SG, Durán N, Nagata N, and Peralta-Zamora P, Semiconductor-assisted photocatalytic degradation of reactive dyes in aqueous solution. Chemosphere. 2000;40:433-440.
47. Habibi MH and Mosavi V, Synthesis and characterization of Fe_2O_3/Mn_2O_3/$FeMn_2O_4$ nano composite alloy coated glass for photo-catalytic degradation of Reactive Blue 222. Journal of Materials Science: Materials in Electronics. 2017;28:11078-11083.
48. Barkaat S, Zuber M, Zia KM, Noreen A, and Tabasum S, UV/H_2O_2/Ferrioxalate Based Integrated Approach to Decolorize and Mineralize Reactive Blue Dye: Optimization Through Response Surface Methodology. Zeitschrift fur Physikalische Chemie. 2021;235:525-547.
49. Li Z, Kang W, Han Z, Yan J, Cheng B, and Liu Y, Hierarchical MnOx@PVDF/MWCNTs tree-like nanofiber membrane with high catalytic oxidation activity. Journal of Alloys and Compounds. 2019;780:805-815.
50. Yaghoubi A, Ramazani A, and Taghavi Fardood S, Synthesis of Al_2O_3/ZrO_2 Nanocomposite and the Study of Its effects on Photocatalytic Degradation of Reactive Blue 222 and Reactive Yellow 145 Dyes. ChemistrySelect. 2020;5:9966-9973.
51. Shojaei Yeganeh M, Kazemizadeh AR, Ramazani A, Eskandari P, and Rabbi Angourani H, Plant-mediated synthesis of $Cu_{0.5}Zn_{0.5}Fe_2O_4$ nanoparticles using Minidium leavigatum and their applications as an adsorbent for removal of reactive blue 222 dye. Materials Research Express. 2019;6:1250f1254.